Clustering process of interstitial atoms in gallium phosphide studied by transmission electron microscopy

Y. Ohno, S. Takeda, and M. Hirata
Department of Physics, Graduate School of Science, Osaka University, 1-16, Machikane-yama, Toyonaka, Osaka 560, Japan
(Received 25 January 1996)

Growth of Frank-type dislocation loops of interstitial type in GaP crystal has been systematically examined by *in situ* transmission electron microscopy to understand the migration of point defects in the crystal. The loops were formed by annealing following 200-keV electron irradiation. Most of the loops were nucleated in the early stage of annealing and the number density of loops remained constant after nucleation. The radius of each loop increased with annealing time and then reached a certain final value. The number density of interstitials aggregated in loops therefore reached a maximum value when the growth of all loops stopped. The maximum density did not depend on annealing temperature but on irradiation conditions (electron dose and irradiation temperature) and it increased quadratically with electron dose. These results were well explained by a proposed model that the loops were formed through the thermal migration of Ga_i-P_i pairs that were introduced during electron irradiation. From the analysis, the migration energy for the interstitial pairs was estimated as 0.9 ± 0.03 eV. [S0163-1829(96)02031-0]

I. INTRODUCTION

Point defects in III-V compound semiconductors have been extensively investigated since they vary the optical and electronic properties of final products even when their concentration is small. For studying the defects, electron irradiation is commonly used since pairs of isolated interstitials and vacancies can be introduced intentionally in a crystal. The structural and dynamical properties of the primary defects have been well described. It is well known that various kinds of defect complexes, such as interstitial clusters, are introduced by annealing after irradiation. Nevertheless, the clustering processes of the point defects have not yet been fully examined.

In GaP, the atomic and electronic structures of a Ga vacancy have been clarified using electron spin resonance[1] and deep-level transient spectroscopy (DLTS).[2] The vacancy is known to be mobile thermally at the temperatures above 700 K.[1,3] The P vacancy has also been studied by positron annihilation spectroscopy[4,5] and theoretical[6] approaches and it is known to migrate thermally above 1100 K. The result of infrared (IR) absorption spectroscopy indicates that the onset temperatures for migration of isolated Ga and P interstitials are 100 K (Ref. 7) and 300 K,[8] respectively.

Above the onset temperature for interstitial migration, two annealing stages of electrical conductivity have been observed in electron-irradiated GaP. The annealing temperatures of the stages are 430 and 530–570 K and they are characterized by two first-order processes with activation energies of 1.5 and 2.0 eV.[9,10] The same annealing stages have been observed by DLTS (Refs. 11 and 12) and thermally stimulated conductivity.[13] Another annealing stage has been observed by IR spectroscopy (about 530 K).[14] These results indicate the existence of several kinds of complexes. However, the structure and annealing of the complexes are still debatable.[12–14]

In the present study, we found the formation of small dislocation loops of interstitial type by annealing following 200-keV electron irradiation. We examined the growth of these interstitial clusters by *in situ* transmission electron microscopy (TEM) under several annealing and irradiation conditions and we concluded that the clusters are formed by thermal migration of interstitial-related complexes that are introduced during electron irradiation.

II. EXPERIMENTS

Specimens were undoped GaP single crystals grown by the Czochralski method. Even though the specimens were nominally undoped, weak photoluminescence emission due to sulfur and oxygen atoms was observed. These impurities were introduced during crystal growth and the concentrations of them may be less than 10^{16} cm^{-3}. Specimens for TEM observation were prepared as follows. Disks with {110} surfaces, 3 mm in diameter and 0.4 mm in thickness, were cut from the crystal using an ultrasonic cutter. The central part of a surface on each disk was dug about 0.32 mm deep and 1 mm in diameter by an ultrasonic drill. Finally, each disk was polished chemically in a mixture of HNO_3 and HCl until a small opening was formed. The crystal around the opening was wedge shaped and suitable for TEM observation.

For introducing Frenkel-type defects intentionally, specimens were irradiated with 200-keV electrons with the electron beam exactly parallel to the ⟨110⟩ direction in a transmission electron microscope (JEOL JEM 2000 EX). The irradiation temperature T_{ir} was kept at 300 K; otherwise it is noted in the text. The irradiation area on a specimen surface was about 2 μm in diameter. After irradiation, the specimens were annealed at a temperature T_{an} (700–1000 K) for a period τ_{an} (0–25 200 s). Due to the thermal drift of a TEM specimen at an elevated temperature, we started to take TEM photographs about 2400 s after the annealing commenced.

Dislocation loops of interstitial type, created by annealing following irradiation, were observed by the weak-beam TEM technique using a 220- or 113-type diffraction spot. The

nucleation of the dislocation loops strongly depended on the irradiation direction of an electron beam with regard to the crystal axis. No loops were formed when the electron beam was inclined by 5° from the ⟨110⟩ direction, since the introduction of point defects was much suppressed by the electron-diffraction-channeling effect.[15] Weak-beam TEM images were taken with the beam of off-axial incident direction. The total electron dose during observation was less than 10^{21} e cm^{-2} and it is smaller than that of irradiation (about 10^{22} e cm^{-2}). Therefore, we could safely neglect the introduction of point defects during TEM observation. We also neglected electron-irradiation-enhanced migration of point defects during TEM observation, since we confirmed that the growth speed of loops with intermittent observation was the same as that with continuous observation.

III. EXPERIMENTAL RESULTS

A. Formation of dislocation loops of interstitial type

Figure 1(a) shows a weak-beam TEM image after electron irradiation (electron flux $\phi_{ir}=5.5\times10^{18}$ cm^{-2} s^{-1} and irradiation period $\tau_{ir}=7200$ s). There is no distinct contrast of lattice defects in the irradiated area [indicated by the circle in Fig. 1(a)]. Figure 1(b) shows the result after subsequent annealing ($T_{an}=1000$ K, $\tau_{an}=1800$ s). A number of defects exist in the irradiated area. The defects were identified as the Frank-type dislocation loop of interstitial type by high-resolution TEM images (Fig. 2). An oblique view of the image along the horizontal direction indicates that the extra {111} plane is inserted. These loops were located homogeneously on four equivalent {111} planes and we did not find another kind of dislocation loop. We found that the loops were formed in an irradiated area after subsequent annealing at the temperature range $T_{an}\geqslant700$ K. It is generally known that the threshold electron energies for atomic displacement of Ga and P atoms in GaP are in the range 100–150 keV,[16] indicating that the electron energy of 200 keV is enough to introduce Frenkel-type defects at both Ga and P sublattices. Therefore, the dislocation loops were formed by the thermal migration of Ga and P interstitials, which are introduced by electron irradiation at 300 K. As reported already, dislocation loops of the same kind are formed in a GaAs crystal by the similar procedure, though the onset temperature for loop formation is slightly higher [773 K (Ref. 17)] than that in GaP. The growth of the loops has not yet been observed *in situ* in GaAs because of rapid deterioration of the specimen surface above 773 K.

We first measured the planar density of the loops in Fig. 1(b) as a function of specimen thickness. As shown in Fig. 3, the density can be fitted with the single straight line that penetrates the origin. This indicates that the volume number density of loops C_L is independent of the specimen thickness and there is virtually no inhomogeneous distribution of loops near surfaces. Therefore, (i) specimen surfaces do not act as a sink of interstitials and (ii) the loops do not originate from contaminant impurity atoms injected under the electron entrance surface. The concentration of interstitials (on the order of 10^{19} cm^{-3}) is much more than that of native impurity atoms in the specimens (less than 10^{16} cm^{-3}). Hence we conclude that the formation of the dislocation loops is an intrinsic bulk phenomenon in a GaP crystal.

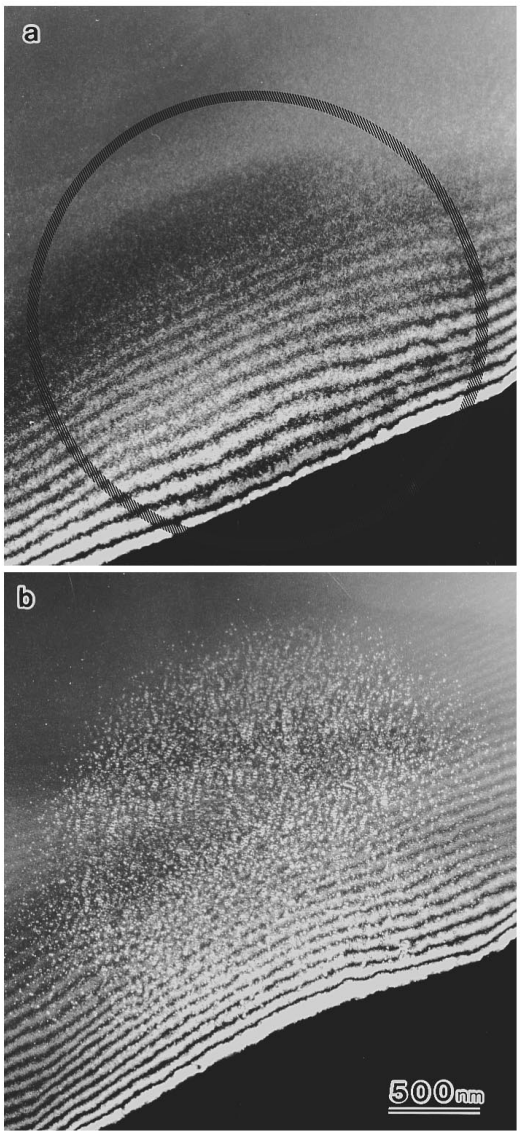

FIG. 1. Weak-beam TEM images of electron irradiated GaP (a) before and (b) after annealing. The irradiated area is about 2 μm in diameter.

B. Nucleation and growth of the dislocation loops by annealing

Growth of the dislocation loops during annealing was pursued by TEM. Figure 4 shows *in situ* TEM images taken at 800 K ($\phi_{ir}=5.5\times10^{18}$ cm^{-2} s^{-1}, $\tau_{ir}=1800$ s). Most loops were nucleated within the annealing time t_{an} of 2400 s and the number density C_L remained constant after the nucleation. The radii r of the loops named a, b, c, and d in Fig. 4 were measured at several t_{an} (Fig. 5). We found that r of the loops are well expressed by a function

$$r=r_0\tanh(At_{an}), \tag{1}$$

where r_0 and A represent the final loop radii and the growth rates, respectively. The values of r_0, A, and r_0A for the best fitted curves indicated in Fig. 5 are summarized in Table I. The products r_0A of the loops are a common value, though r_0 and A of each loop are slightly different. We found that the ratio of the standard deviation of r_0 to the average of r_0 is about 6/100.

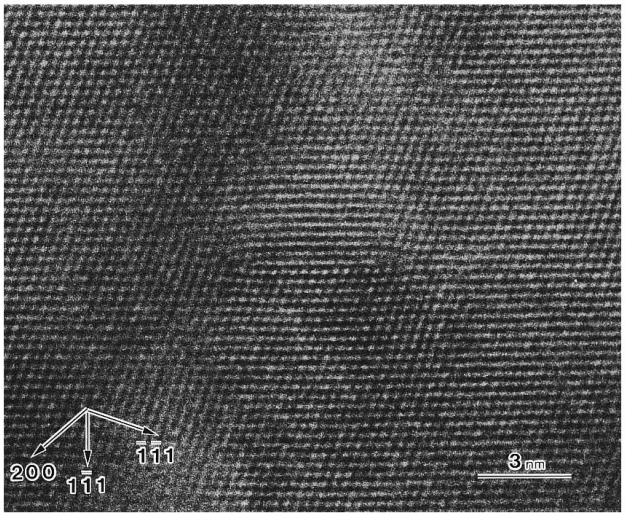

FIG. 2. High-resolution TEM image of a Frank loop of interstitial type taken with the ⟨110⟩ incidence.

The growth of loops was observed *in situ* at various T_{an} (700, 725, 750, 775, and 800 K) and we found that r is well described by Eq. (1). The product r_0A depended only on T_{an} and increased with rising T_{an} (Table II). We could not estimate A in the temperature range $T_{an}>800$ K since the growth of loops stopped within a short period less than 2400 s.

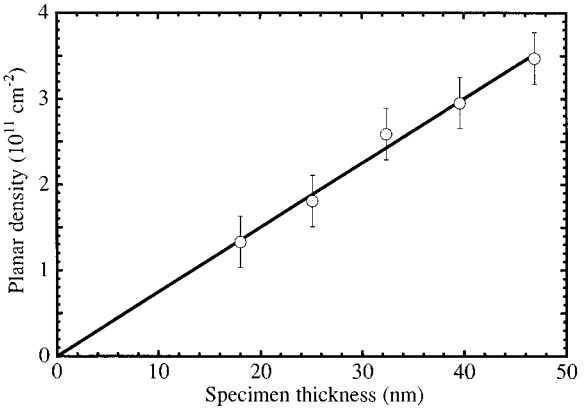

FIG. 3. Planar density of loops against specimen thickness. The density is proportional to the specimen thickness, indicating that the volume number density is independent of the thickness.

C. Number density of the dislocation loops

Figure 6 shows $\ln(C_L)$ vs $1/kT_{an}$. C_L was measured after all loops were nucleated. The electron flux ϕ_{ir} was 5.5×10^{18} cm^{-2} s^{-1} and irradiation periods τ_{ir} were 3000 s (open and closed circles) and 1500 s (squares). As shown in Fig. 6, C_L increases exponentially with $1/kT_{an}$. The slopes of the straight lines in Fig. 6 provide the energies of 0.47 eV (open circles) and 0.45 eV (squares). The closed circles in Fig. 6 were measured in a specimen that was annealed stepwise at

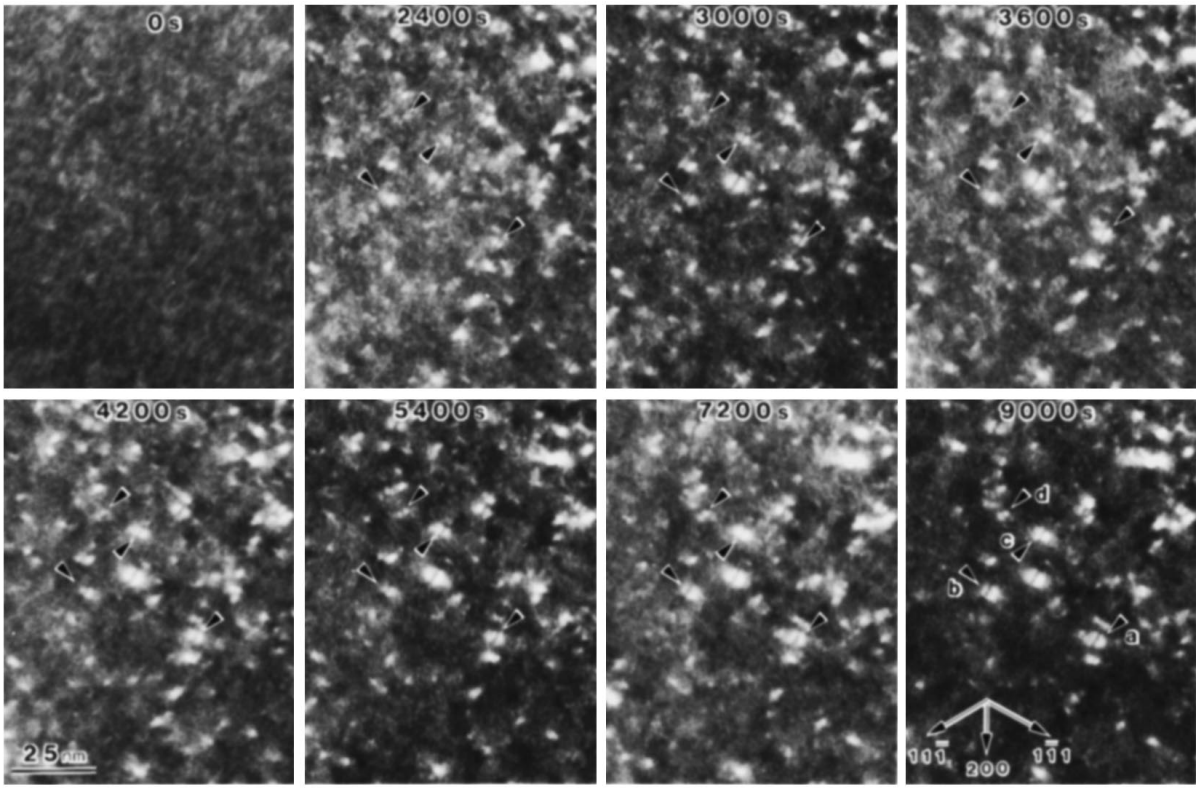

FIG. 4. Growth of the dislocation loops observed *in situ* by TEM at the annealing temperature $T_{an}=800$ K.

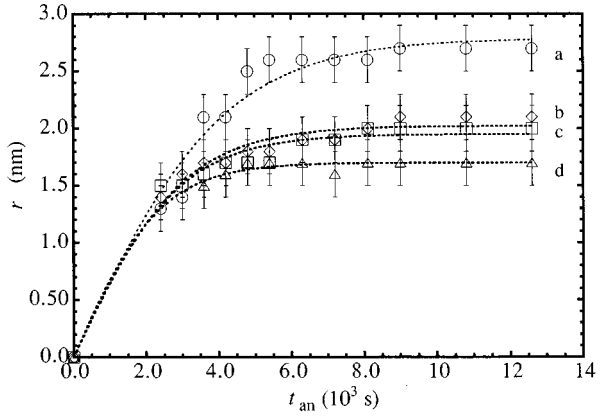

FIG. 5. Variation of loop radii r measured in Fig. 4 as a function of annealing time t_{an}

700, 900, and 1000 K. In the step-annealing process, loops occasionally shrunk and released interstitials, which then took part in another loop. The estimated energy in Fig. 6 (0.53 eV) differs from those in the constant temperature annealing.

D. Number density of agglomerated interstitials in the dislocation loops

The volume number density of Ga and P interstitials aggregated in all the loops C_{IL} can be estimated by a simple formula

$$C_{IL}=\frac{2}{V}\sum_i \pi r_i^2\sigma, \tag{2}$$

in which V represents the specimen volume irradiated by electrons, σ is a planar density of Ga or P interstitials in the Frank-type loops (1.5×10^{15} cm^{-2}), and the i's denote individual loops. C_{IL} reached a maximum value $C_{IL}(\infty)$ when the growth of all loops stopped. Figure 7 shows $C_{IL}(\infty)$ as a function of T_{an}. The irradiation and annealing condition were the same as those used in Fig. 6. The symbols have the same meaning as in Fig. 6. As shown in Fig. 7, $C_{IL}(\infty)$ is independent of T_{an} on the condition of constant τ_{ir}. Moreover, $C_{IL}(\infty)$ in the step annealing is the same as that in the constant temperature annealing when τ_{ir} is the same. Figure 8 summarizes $C_{IL}(\infty)$ vs electron dose D; ϕ_{ir} is multiplied by τ_{ir}. These results lead us to the important fact that $C_{IL}(\infty)$ is independent of ϕ_{ir}, τ_{ir}, and T_{an} under the constant dose D. As seen in Fig. 8, $C_{IL}(\infty)$ increases quadratically with increasing electron dose in the range $D\leqslant2\times10^{22}$ cm^{-2}. This is a characteristic trend in the second-order reaction, suggesting

TABLE I. Fitting parameters of Fig. 5.

Loops	r_0 (nm)	A (s^{-1})	r_0A (nm s^{-1})
a	2.8	4.8×10^{-4}	1.3×10^{-3}
b	2.0	6.6×10^{-4}	1.3×10^{-3}
c	1.9	6.9×10^{-4}	1.3×10^{-3}
d	1.7	8.4×10^{-4}	1.4×10^{-3}

TABLE II. Fitting parameters at several annealing temperatures.

T_{an} (K)	r_0A (nm s^{-1})
700	2.5×10^{-4}
725	3.9×10^{-4}
750	9.9×10^{-4}
775	1.1×10^{-3}
800	1.3×10^{-3}

that the loops are formed through the migration of interstitial pairs, that is, the pairs of Ga and P interstitials. Details are discussed in the next section.

Figure 9 shows the variation of $C_{IL}(\infty)$ with the irradiation temperature T_{ir}. Specimens were irradiated with $D=4.0\times10^{22}$ e cm^{-2} and subsequently annealed at $T_{an}=1000$ K. $C_{IL}(\infty)$ reaches the maximum at $T_{ir}=300$ K and decreases rapidly with raising T_{ir}.

IV. DISCUSSION

A. Rate equations based on the migration of isolated interstitials

We have shown that the formation of dislocation loops is an intrinsic bulk phenomenon in GaP crystals. Since we confirmed that dispersion of the radii of all the loops is small, we may replace r by the average radius $\tilde{r}$ and rewrite Eq. (2) as

$$C_{IL}=2\pi\tilde{r}^2\sigma C_L. \tag{3}$$

Therefore, we apply the chemical kinetics theory, in which the homogeneous distribution of defects is usually assumed. Dislocation loops of interstitial type are formed in various metals and alloys during electron irradiation and the nucleation and growth of them have been well understood by the interaction of point defects. Before we discuss the results in GaP, let us recall the standard rate equations that apply to metals and alloys.[18] We consider the phenomena at low T_{ir} at

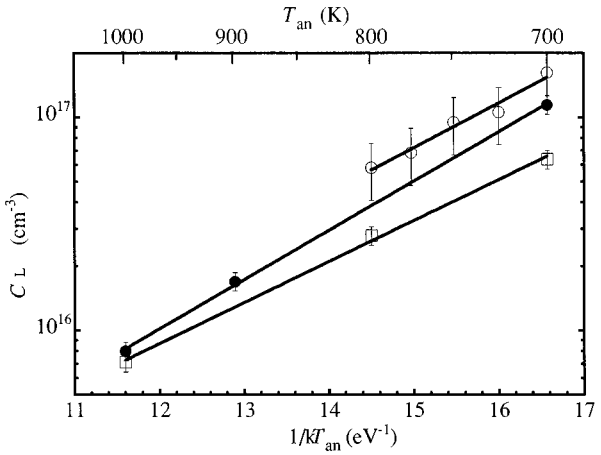

FIG. 6. Logarithms of the density of loops C_L against the reciprocal of annealing temperature $1/kT_{an}$. The irradiation period $\tau_{ir}=3000$ s (open and closed circles) and 1500 s (open squares), respectively. The closed circles represent the results of a specimen that underwent the step annealing.

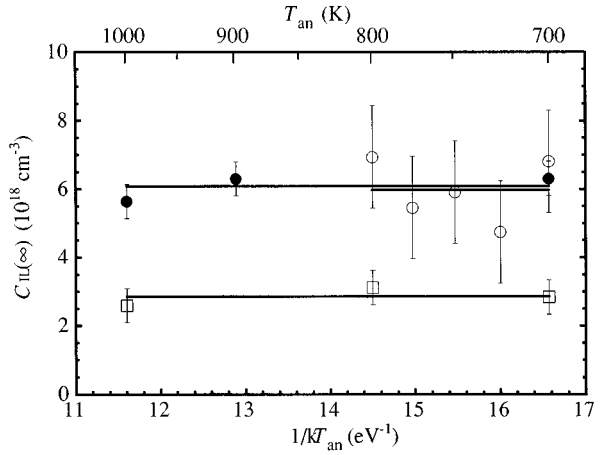

FIG. 7. Final density of aggregated interstitials $C_{IL}(\infty)$ against the reciprocal of annealing temperatures $1/kT_{an}$. The irradiation period τ_{ir}=3000 s (open and closed circles) and 1500 s (open squares), respectively. The closed circles represent the results of a specimen that underwent the step annealing.

which only interstitials can freely migrate thermally. Point defects introduced by irradiation annihilate when interstitials jump into the recombination volume around vacancies. Therefore the change of the concentration of interstitials C_I and vacancies C_V can be expressed as

$$\frac{dC_I}{dt}=\frac{dC_V}{dt}=P-ZMC_IC_V, \tag{4}$$

where P is the production rates of Frenkel defects, M the mobility of interstitials, and Z the number of capture sites around a vacancy for interstitials. Dislocation loops of interstitial type, of course, act as sinks for interstitials. The additional term of variation of C_I is represented as

$$-(2\pi\tilde{r}\alpha)MC_LC_I, \tag{5}$$

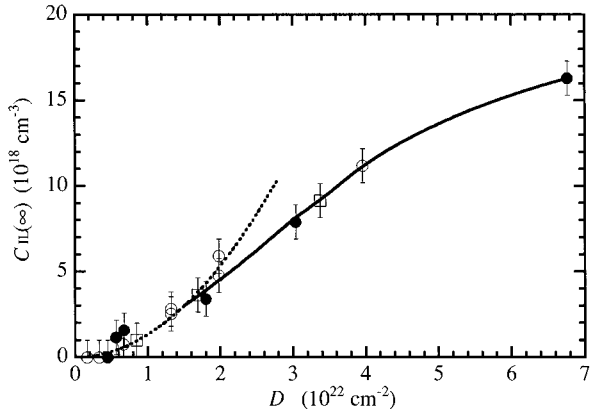

FIG. 8. Final density $C_{IL}(\infty)$ as a function of the electron dose D. Open symbols (circles and squares), $\phi_{ir}=5.5\times10^{18}$ cm^{-2} s^{-1}; filled symbols (circles), τ_{ir}=1800 s, circles (open and filled), T_{an}=1000 K; squares (open), T_{an}=950 K.

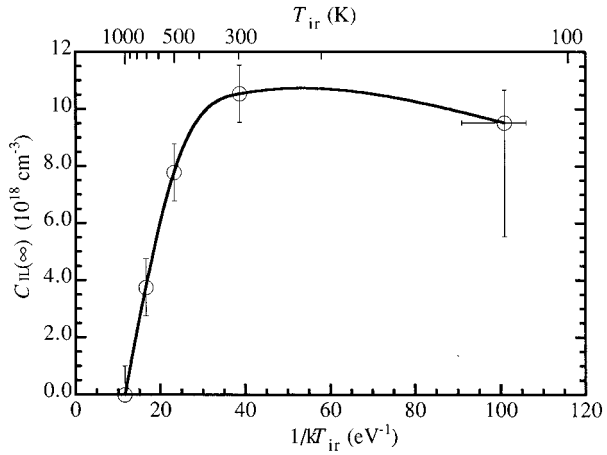

FIG. 9. Variation of the final density of aggregated interstitials $C_{IL}(\infty)$ with several irradiation temperatures T_{ir}.

where α represents the capture site number per unit length around a loop for the interstitials. The mobility M can be estimated by measuring the variation of $\tilde{r}$ and C_L as a function of P and T_{ir}.[18]

B. Extended rate equations based on the migration of Ga_i-P_i pairs

The above-mentioned model is insufficient to explain the present experiments in GaP. First, the onset temperature for formation of loops (700 K) was much higher than that for migration of isolated Ga [about 100 K (Ref. 7)] and P [about 300 K (Ref. 8)] interstitials. This suggests that the loops were formed by migration of not isolated interstitials but interstitial-related complexes. Second, the model yields the result that $C_{IL}(\infty)$ increases linearly with D, while the observed $C_{IL}(\infty)$ increases quadratically as given in Fig. 8. Since the quadratic dependence of $C_{IL}(\infty)$ indicates that the complexes, which are agglomerated in the loops, are formed in the second-order reaction, we have come to consider that the complexes are Ga_i-P_i interstitial-pairs. For a quantitative understanding of the growth of loops, we propose the extended model as depicted in the equations

$$\frac{dC_{I(\xi)}}{dt}=P_{(\xi)}-Z_{(\xi)}M_{(\xi)}C_{I(\xi)}C_{V(\xi)} -Z_{II}(M_{(\mathrm{Ga})}+M_{(\mathrm{P})})C_{I(\mathrm{Ga})}C_{I(\mathrm{P})}, \tag{6}$$

$$\frac{dC_{V(\xi)}}{dt}=P_{(\xi)}-Z_{(\xi)}M_{(\xi)}C_{I(\xi)}C_{V(\xi)}, \tag{7}$$

$$\frac{dC_{II}}{dt}=Z_{II}(M_{(\mathrm{Ga})}+M_{(\mathrm{P})})C_{I(\mathrm{Ga})}C_{I(\mathrm{P})}-(2\pi\tilde{r}\alpha)M_{II}C_LC_{II}, \tag{8}$$

$$\frac{dC_{IL}}{dt}=(2\pi\tilde{r}\alpha)M_{II}C_LC_{II}. \tag{9}$$

$C_{I(\xi)}$ and $C_{V(\xi)}$ represent the concentration of isolated interstitials and vacancies, respectively. $P_{(\xi)}$ is the production rate of Frenkel defects and is equal to zero during annealing. $M_{(\xi)}$

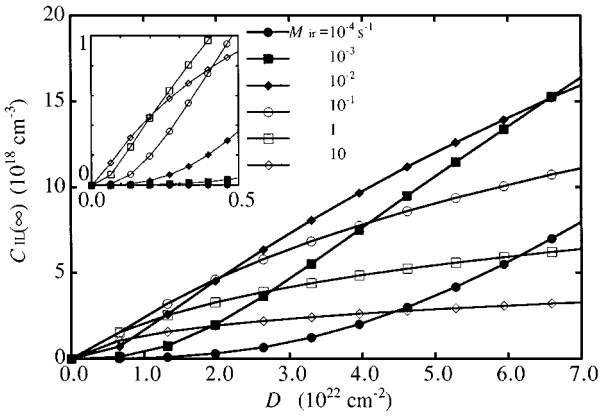

FIG. 10. Variation of the simulated final density $C_{IL}(\infty)$ with several electron doses D and interstitial mobilities $M_{\rm ir}$. $M_{\rm ir}$ in the computations are written in the figure. It is assumed that the pairs are formed only by irradiation.

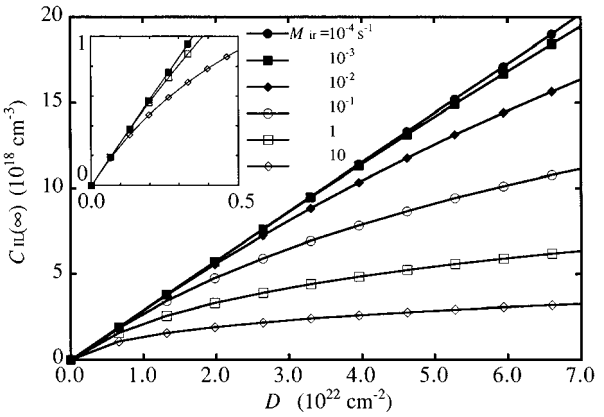

FIG. 11. Variation of the simulated final density $C_{IL}(\infty)$ using the same parameters as those assumed in Fig. 10. It is assumed that the pairs are formed during both irradiation and annealing.

is the mobility of interstitials. ξ denotes the species of atoms Ga and P. $Z_{(\xi)}$ represents the number of capture sites around a ξ vacancy for ξ interstitials. Instead of the term (5), we add the third term in Eq. (6), which represents the rate of the disappearance of isolated interstitials by the formation of the interstitial pair. The pair is formed when an interstitial jumps into the spontaneous combination volume around an interstitial of the other kind. Z_{II} denotes the number of capture sites of the interstitial pairing. The variation of the concentration of the pairs C_{II} is described in Eq. (8). The second term in Eq. (8) represents the rate of the disappearance of the pairs by the formation of the loops, where M_{II} represents the mobility of the pairs. In Eq. (9), dislocation loops of interstitial type are formed by migration of the pairs. Since the vacancies are generally immobile below 700 K (Ga) (Refs. 1 and 3) and 1100 K (P),[4] the clustering of Ga and P vacancies is neglected. Another assumption is that coupled Ga and P interstitials never combine with an isolated single Ga or P vacancy. By this assumption, the experimental results that $C_{IL}(\infty)$ is independent of annealing temperatures (Sec. III D) can be easily explained.

C. Interpretation of the experimental results

1. Formation of Ga_i-P_i pairs

Numerical calculations of the rate equations (6)–(9) were performed with several sets of parameters. In the following computations, we naturally assumed that $P_{(\rm Ga)}=P_{(\rm P)}=10^{-6}$ s^{-1} during irradiation, $P_{(\rm Ga)}=P_{(\rm P)}=0$ s^{-1} during annealing, $Z_{(\rm Ga)}=Z_{(\rm P)}=10^2$, and the concentrations of point defects before irradiation were assumed to be zero. We assumed that $M_{(\rm Ga)}=M_{(\rm P)}(=M_{\rm ir})$ and $M_{II}=0$ during irradiation, and $M_{(\rm Ga)}=M_{(\rm P)}(=M_{\rm an})$ during annealing. First, we confirmed that, in our model, $C_{IL}(\infty)$ is independent of both $M_{\rm an}$ and M_{II} on the condition of constant D and $M_{\rm ir}$. This reproduces the experiment shown in Fig. 7, since $M_{\rm an}$ and M_{II} are related to the annealing temperature $T_{\rm an}$.

Figure 10 shows the simulated curves of $C_{IL}(\infty)$ vs D in which we assumed that the pairs are created only by electron irradiation: $Z_{II}=4$ during irradiation and $Z_{II}=0$ during annealing. $C_{IL}(\infty)$ increases quadratically with D in the lower dose range; $C_{IL}(\infty)$ computed with $M_{\rm ir}=10^{-2}$ s^{-1} agrees well with the measurement shown in Fig. 8. At a certain dose, simulated $C_{IL}(\infty)$ varies with $M_{\rm ir}$. In the range of lower mobility, the density $C_{IL}(\infty)$ increases with increasing $M_{\rm ir}$ and in the range of higher mobility, the $C_{IL}(\infty)$ decrease rapidly as the value $M_{\rm ir}$ increases. The variation of $M_{\rm ir}$ is related to that of $T_{\rm ir}$; $M_{\rm ir}$ is small when $T_{\rm ir}$ is low. Therefore, the dependence of simulated $C_{IL}(\infty)$ on $T_{\rm ir}$ is consistent with the experiments shown in Fig. 9. Similar results could be obtained whenever the values of Z_{II}, $Z_{(\xi)}$, and $P_{(\xi)}$ were on the order of 10^0, 10^2, and 10^{-6} s^{-1}, respectively.

We next considered an alternative model in which the interstitial pairs were formed during not only irradiation but also annealing: $Z_{II}=4$ during both irradiation and annealing. Figure 11 shows the simulated curves of $C_{IL}(\infty)$ vs D using the same parameters as those assumed in Fig. 10. The simulated $C_{IL}(\infty)$ increases linearly with D. It decreases monotonically with $M_{\rm ir}$ at a certain D. Consequently, the experimental data are consistently described by the former model: the interstitial pairs are created only by electron irradiation.

2. Growth of dislocation loops

We found that an interesting formula consisting of some observable parameters and the mobility M_{II} is valid during annealing. After the nucleation of all loops, the number density of loops C_L was constant during annealing (Sec. III C). From Eqs. (3) and (9), the variation of averaged radius $\tilde{r}$ is written as

$$\frac{d\tilde{r}}{dt_{\rm an}}=\frac{\alpha M_{II}}{2\sigma}\,C_{II}. \tag{10}$$

The first term of Eq. (8) can be omitted because the interstitial pairs were not formed during annealing. Combining Eqs. (8) and (10), $C_{II}=C_{II}(\tau_{\rm ir})$ and $\tilde{r}=0$ at $t_{\rm an}=0$, we can obtain the analytical formula of $\tilde{r}$,

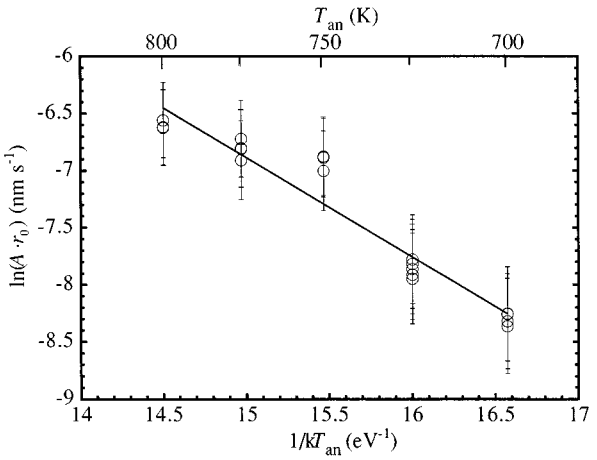

FIG. 12. Arrhenius plot of the product of the final loop radius and growth rate r_0A.

$$\tilde{r}=\left\{\frac{C_{II}(\tau_{ir})}{2\pi\sigma C_L}\right\}^{0.5}\tanh\left\{\alpha M_{II}\left(\frac{\pi C_L C_{II}(\tau_{ir})}{2\sigma}\right)^{0.5}t_{an}\right\}. \tag{11}$$

This result exactly corresponds to the experiments represented by Eq. (1). The product r_0A in Eq. (1) is therefore written as

$$r_0A=\frac{\alpha C_{II}(\tau_{ir})}{2\sigma}M_{II}. \tag{12}$$

Since α, $C_{II}(\tau_{ir})$, and σ are independent of T_{an}, the variation of r_0A with T_{an} arises from the temperature dependence of M_{II}.

D. Migration energy for interstitial pairs

We estimated the migration energy for interstitial pairs using Eq. (12). Figure 12 shows the Arrhenius plot of the product r_0A with T_{an}. The slope of the straight line provides the migration energy of 0.87 eV. This value well agrees with one obtained by Hirata, Hirata, and Kiritani (0.9 eV),[19] even though they claimed that the energy was related to the mobility of isolated interstitials. Using a high-voltage TEM technique, they plotted $\ln(C_L)$ vs $1/kT_{ir}$ and estimated the migration energy as twice the energy shown by the slope of the logarithm.[19] Suppose the loops were formed by clustering of interstitial pairs introduced by irradiation; the energy obtained by them is replaced with one for interstitial pairs. The same analysis may apply to our experimental results denoted in Fig. 6. The migration energies for the interstitial pairs are estimated to be 0.93 eV (open circles) and 0.90 eV (open squares), which are almost the same as the one estimated in Fig. 12. The estimated energy for step-annealing experiments, 1.06 eV (closed circles), differs from the one in Fig. 12. In the case of step annealing, interstitial pairs agglomerated in loops after annealing of the first step. Some loops released the pairs during annealing of the second step and thus the concentration of the pairs around the loops was heightened. Since the pairs distributed inhomogeneously, the chemical kinetics theory is inapplicable to this case. Consequently, the migration energy for interstitial pairs is estimated as 0.9 ± 0.03 eV.

E. Onset temperature for the migration of interstitial pairs

We observed the formation of dislocation loops above 700 K. Interstitial clusters whose size is less than 1 nm may be formed by annealing below 700 K, though they are hardly observable by TEM. Suppose the relationships between C_L and T_{an} denoted in Fig. 6 and between $C_{IL}(\infty)$ and T_{an} in Fig. 7 are held even at low T_{an}: we can estimate C_L and $C_{IL}(\infty)$ at the temperature range $T_{an}<700$ K. At $T_{an}=530$–540 K, C_L reaches a quarter of $C_{IL}(\infty)$; only two interstitial pairs are contained in a loop. This temperature corresponds to the onset temperature for the migration of the interstitial pairs. The estimated temperature is much higher than the onset temperature for migration of isolated Ga and P interstitials [100 K (Ref. 7) and 300 K (Ref. 8)] and lower than that of isolated Ga and P vacancies [700 K (Refs. 1–3) and 1100 K (Ref. 5)].

The onset temperature for the pair migration is close to the annealing temperature of DLTS spectra in electron-irradiated GaP (Refs. 11 and 12) (530–570 K). It is suggested that these spectra correspond to electron traps: the energy levels of the pairs of P interstitial and P vacancy.[12] The annealing of the defects is attributed to the migration of P interstitials. The estimated onset temperature is also close to an annealing temperature of IR spectra in electron-irradiated GaP (530 K).[14] According to the work, these spectra correspond to the local vibrational mode of a P atom on a Ga site (antisite defect[14]) and the annealing mechanism of this defect is still uncertain. The annealing of the defects observed in DLTS and IR spectra may be related to the migration of interstitial pairs, though it is possible that different kinds of defects anneal at the same temperature as observed in GaAs.[20]

V. CONCLUSION

We found that Frank loops of interstitial type are formed uniformly in GaP crystal by annealing following 200-keV electron irradiation. The results of *in situ* TEM observations showed that the loops are formed through the two processes: (i) introduction of point defects by irradiation and (ii) thermal migration of point defects by annealing.

The loop radius increased as a function of annealing temperatures T_{an}. As T_{an} raised, the volume number density of loops C_L decreased. The final density of agglomerated interstitials in all loops $C_{IL}(\infty)$ only depended on irradiation conditions (electron dose D and irradiation temperature T_{ir}) and increased quadratically with D. These results are well explained by a proposed model that the loops were formed through the thermal migration of Ga_i-P_i pairs that were introduced during electron irradiation. From the analysis, the migration energy for the interstitial pairs is estimated as 0.9 ± 0.03 eV.

ACKNOWLEDGMENT

This work was supported in part by a Grant-in-Aid for Scientific Research from the Ministry of Education, Science and Culture, Japan.

[1] T. A. Kennedy and N. D. Wilsey, Phys. Rev. B **23**, 6585 (1981).
[2] P. M. Mooney, T. A. Kennedy, and M. B. Small, Physica B+C **116B**, 431 (1982).
[3] B. Zhou, J. Fong, and J. Huang, Phys. Status Solidi **102**, 533 (1987).
[4] G. Dlubek, O. Brümmer, and A. Polity, Appl. Phys. Lett. **49**, 385 (1986).
[5] F. Dominguez-Adame, J. Piqueras, N. de Diego, and P. Moser, Solid State Commun. **67**, 665 (1988).
[6] J. A. Van Vechten, J. Electron. Mater. **4**, 1159 (1975).
[7] S. R. Morrison, R. C. Newman, and F. J. Thompson, J. Phys. C **5**, L46 (1972).
[8] S. R. Morrison and R. C. Newmann, J. Phys. C **6**, L223 (1973).
[9] E. Yu. Brailovski, I. D. Konozenko, and V. P. Tartachnik, Fiz. Tekh. Poluprovodn. **9**, 769 (1975) [Sov. Phys. Semicond. **9**, 505 (1975)].
[10] E. Yu. Brailovski, G. N. Erisyan, and V. P. Tartachnik, Fiz. Tekh. Poluprovodn. **9**, 1805 (1975) [Sov. Phys. Semicond. **9**, 1187 (1975)].
[11] D. V. Lang and L. C. Kimerling, Appl. Phys. Lett. **28**, 248 (1976).
[12] M. A. Zaidi, M. Zazoui, and J. C. Bourgoin, J. Appl. Phys. **74**, 4948 (1993).
[13] E. Yu. Brailovski and N. D. Marchuk, Phys. Status Solidi **58**, 41 (1980).
[14] R. C. Newmann, in *Defects in Semiconductors 14*, edited by L. C. Kimerling and J. M. Parsey, Jr. (The Metallurgical Society of AIME, Coronado, CA, 1984), p. 87.
[15] K. Urban and N. Yoshida, Radiat. Eff. **42**, 144 (1979).
[16] R. M. Esposito and J. J. Loferski, in *Proceedings of IXth International Conference on the Physics of Semiconductors*, edited by S. M. Ryvkin (Nauka, Moscow, 1968), p. 1105.
[17] J. H. Neethling, in *Proceedings of the 13th International Congress on Electron Microscopy*, edited by B. Jouffrey and C. Colliex (Les Editions de Physique, Les Ulis, 1994), p. 101.
[18] M. Kiritani, J. Nucl. Matter **216**, 220 (1994).
[19] M. Hirata, M. Hirata, and M. Kiritani, in *Proceedings of International Symposium on Behavior of Lattice Imperfections in Materials—In situ Experiments with HVEM*, edited by H. Fujita (Research Center for Ultra-high Voltage Electron Microscopy, Osaka, 1985), p. 199.
[20] P. M. Moony, F. Pourin, and J. C. Bourgoin, Phys. Rev. B **28**, 3372 (1983).